

## Mapping of Subunit–Subunit Contact Surfaces on the $\beta$ Subunit of *Escherichia coli* RNA Polymerase<sup>†</sup>

Tasuku Nomura,<sup>‡,§</sup> Nobuyuki Fujita,<sup>‡</sup> and Akira Ishihama<sup>\*,‡</sup>

Department of Molecular Genetics, National Institute of Genetics, and School of Life Science, Graduate University for  
Advances Studies, Mishima, Shizuoka 411-8540, Japan

Received October 5, 1998; Revised Manuscript Received November 23, 1998

**ABSTRACT:** The RNA polymerase core enzyme of *Escherichia coli* is composed of  $2\alpha$ ,  $1\beta$ , and  $1\beta'$  subunits. Previously we mapped the  $\alpha$ – $\alpha$ ,  $\alpha$ – $\beta$ , and  $\alpha$ – $\beta'$  contact sites on the  $\alpha$  subunit. Here we analyzed the  $\alpha$  subunit contact sites on the  $\beta$  subunit by using various experimental approaches: (i) comparison of the proteolytic cleavage map between the unassembled free  $\beta$  subunit and the  $\alpha_2\beta$  complex; (ii) analysis of the binary complex formation between His<sub>6</sub>-tagged intact  $\alpha$  subunit and various truncated  $\beta$  fragments; and (iii) analysis of the complex formation between the  $\alpha$  subunit and various His<sub>6</sub>-tagged  $\beta$  fragments. The results altogether indicate that two regions of the  $\beta$  subunit are involved in the full activity of  $\alpha$  binding, that is, the primary contact site between residues 737 and 904 and the secondary region with assembly control activity downstream from residue 1138. All of the  $\alpha$  subunit– $\beta$  fragment binary complexes identified in this study were found to bind  $\beta'$  subunit and form pseudo-core complexes, indicating that the regions of  $\beta$  involved in  $\alpha$  subunit contact also participate in interaction with the  $\beta'$  subunit.

The RNA polymerase holoenzyme of *Escherichia coli* is composed of the core enzyme with the subunit composition of  $\alpha_2\beta\beta'$  and one of seven different species of the  $\sigma$  subunit. The core enzyme carries all of the enzymatic activities for RNA polymerization, but the  $\sigma$  subunit is required for the recognition of promoters and accurate initiation from the promoters. The core enzyme is assembled sequentially both in vitro and in vivo in the order:  $2\alpha \rightarrow \alpha_2 \rightarrow \alpha_2\beta \rightarrow \alpha_2\beta\beta'$  (premature core)  $\rightarrow$  E (active core) (reviewed in ref 1). Since the  $\beta$  and  $\beta'$  subunits do not form stable binary complexes under isolated states (2) [these two subunits contact each other in the assembled RNA polymerase], the  $\alpha$  subunit is considered to play a key role in the RNA polymerase assembly by providing the contact surfaces for both  $\beta$  and  $\beta'$  subunits. In the assembled core enzyme, one  $\alpha$  subunit contacts with the  $\beta$  subunit while the other  $\alpha$  makes direct contact with the  $\beta'$  subunit (3).

Genetic and biochemical studies indicated that the subunit–subunit contact sites on  $\alpha$ , including the sites for  $\alpha$  dimerization and the contact sites with the  $\beta$  and  $\beta'$  subunits, are all located within the amino(N<sup>1</sup>)-terminal domain (NTD) down to residue 235 (4–6), whereas the carboxy(C)-terminal domain (CTD) is involved in transcription regulation through

direct interactions with class-I (or  $\alpha$  contact) transcription factors and DNA UP elements (ref 5; also reviewed in refs 7–9). These two functional domains form independent structural domains (10–13), each being connected by a long flexible linker (14). Previously, we performed detailed mapping of the  $\alpha$ – $\alpha$ ,  $\alpha$ – $\beta$ , and  $\alpha$ – $\beta'$  contact sites on the  $\alpha$  subunit by making a number of  $\alpha$  mutants with deletion, insertion, and Ala substitution mutations (15–17). The contact sites within  $\alpha$  dimers were further analyzed by mapping the cleavage sites in  $\alpha$  by a chemical protease conjugated at various positions of the  $\alpha$  subunit (18).

On the contrary, relatively little is known on the subunit–subunit contact sites on the two large subunits,  $\beta$  and  $\beta'$ . In this report, we describe the map of  $\alpha$  subunit contact sites on the  $\beta$  subunit determined using two approaches: analysis of the proteolytic cleavage pattern of the unassembled free  $\beta$  subunit and the intermediate subassembly  $\alpha_2\beta$  complex; and analysis of the complex formation between various  $\beta$  fragments and the hexahistidine (His<sub>6</sub>)-tagged  $\alpha$  subunit or between various His-tagged  $\beta$  fragments and the intact  $\alpha$  subunit. The results herein described generally agree with the recent findings by Wang et al. (19), who analyzed the  $\alpha$  subunit contact site on the  $\beta$  subunit by limited proteolysis of the  $\alpha_2\beta$  complex and binding assay of  $\beta$  fragments to the N-terminal domain of  $\alpha$  subunit. These authors proposed that the primary contact site is located in the C-terminal-proximal region of the  $\beta$  subunit. However, we propose that the primary and tight contact site of  $\alpha$  subunit is located in the central portion of  $\beta$  polypeptide and the C-terminal-proximal region is needed as the secondary and possibly regulatory site for either efficient binding of the  $\alpha$  subunit or stabilization of the  $\alpha$ – $\beta$  contact.

<sup>†</sup> This work was supported by Grants from the Ministry of Education, Science, Sports, and Culture of Japan, and CREST (Core Research for Evolutional Science and Technology) of Japan Science and Technology Corporation (JST).

<sup>\*</sup> To whom correspondence should be addressed. Phone: 81-559-81-6741. Fax: 81-559-81-6746. E-mail: aishihama@lab.nig.ac.jp.

<sup>‡</sup> National Institute of Genetics.

<sup>§</sup> Graduate University for Advanced Studies.

<sup>1</sup> Abbreviations: N-, amino-; C-, carboxy-; DTT, dithiothreitol; SDS, sodium dodecyl sulfate; PAGE, polyacrylamide gel electrophoresis; PMSF, phenylmethylsulfonyl fluoride; PVDF, poly(vinylidene difluoride).

Table 1: Construction of Expression Plasmids for  $\beta$  Fragments

plasmid	<i>rpoB</i> segment <sup>a</sup>	insertion site on pET21d <sup>b</sup>
pETB[1–1318]-CH <sub>6</sub>	<i>NdeI-SphI</i>	<i>NdeI-XhoI</i>
pETB[1–1138]-CH <sub>6</sub>	<i>NdeI-NruI</i>	<i>NdeI-XhoI</i>
pETB[1–936]-CH <sub>6</sub>	<i>NdeI-NruI</i>	<i>NdeI-XhoI</i>
pETB[1–736]-CH <sub>6</sub>	<i>NdeI-HpaI</i>	<i>NdeI-HpaI</i>
pETB[1–434]-CH <sub>6</sub>	<i>NdeI-EcoRV</i>	<i>NdeI-XhoI</i>
pETB[445–1342]-CH <sub>6</sub>	<i>EcoRV-SacI</i>	<i>NcoI-SacI</i>
pETB[737–1342]-CH <sub>6</sub>	<i>HpaI-SacI</i>	<i>NcoI-SacI</i>
pETB[737–1138]-CH <sub>6</sub>	<i>HpaI-NruI</i>	<i>NcoI-XhoI</i>
pETB[737–936]-CH <sub>6</sub>	<i>HpaI-NruI</i>	<i>NcoI-NotI</i>
pETB[937–1342]-CH <sub>6</sub>	<i>SacI-NruI</i>	<i>NheI-SacI</i>
pETB[937–1138]-CH <sub>6</sub>	<i>NruI-NruI</i>	<i>NheI-XhoI</i>
pETB[1014–1342]-CH <sub>6</sub>	<i>PvuII-SacI</i>	<i>NcoI-SacI</i>

<sup>a</sup> The *rpoB* gene was treated with the indicated restriction enzymes.

<sup>b</sup> The isolated *rpoB* fragments fused with the sequence for His<sub>6</sub>-tag were inset into pET vector between the indicated enzyme sites.

All of the  $\beta$  fragment– $\alpha$  binary complexes isolated in this study were able to bind  $\beta'$  subunit leading to form pseudo-core complexes, suggesting that the  $\beta'$  subunit contact site(s) on the  $\beta$  subunit is(are) located near the  $\alpha$  contact sites.

## EXPERIMENTAL PROCEDURES

**Construction of Expression Plasmids.** pGEMEX-1 (Promega) is used as an expression vector of foreign proteins in *E. coli* as fusions with the phage T7 gene 10 segment. For the construction of expression vector pGET of intact proteins without the fusion, pGEMEX-1 (Promega) was treated with *Bgl*II and *Hind*III to remove a segment of the phage T7 gene 10 sequence and then a *Bgl*II–*Hind*III fragment from pET21b (Novagen) containing multi-cloning sites and the T7 promoter was inserted between the *Bgl*II and *Hind*III sites.

For the construction of plasmid pPNE2017, an *EheI*–*Ssp*I fragment of the *rpoBC* operon was inserted, after addition of *Bam*HI linker sequence at both ends, into pET3a vector at the *Bam*HI site. For the construction of pGETBC [the  $\beta$  and  $\beta'$  expression plasmid], the *rpoBC* *Bam*HI fragment was re-isolated from pPNE2017 and inserted into the *Bam*HI site of pGET (see above). For the construction of pGETB [the  $\beta$  expression plasmid], pGETBC was digested with *Sph*I and *Sac*I to remove the *rpoC* coding sequence. Because this *Sph*I–*Sac*I digestion resulted in truncation of the *rpoB* sequence at its C-terminal-proximal region, the missing region was amplified by PCR using a pair of 5' and 3' primers with the sequence of (5')GTCTGACGTGAACGGTC(3') and (5')-CCTGTTTGAGCTCGAATTACTCG(3'), respectively, and the PCR product was treated with *Sph*I and *Sac*I and ligated into pGETBC between *Sph*I and *Sac*I. For construction of pGETB–CH<sub>6</sub> [the expression plasmid of His<sub>6</sub>-tagged  $\beta$  subunit at its C-terminus], a sequence encoding His<sub>6</sub>-tag was PCR-amplified using the above 5' primer and a 3' primer with the sequence of TGTCGAGCTCTTAGTGGTGGTG-GTGGTGGTGCTCGTCTTCCAGTTCG and, after treatment with *Sph*I and *Sac*I, inserted into pGETB between *Sph*I and *Sac*I.

For the construction of expression vectors for various  $\beta$  fragments fused to His<sub>6</sub>-tag, each *rpoB* fragment was isolated by treatment with various restriction enzymes, as described in Table 1, and inserted into pET21 at the respective multi-cloning sites, as specified in Table 1, located downstream of the T7 promoter. All of the insertion sites except for the

*Sac*I site were blunt-ended by treatment with T4 polymerase or *S*I nuclease as to match the reading frame and to introduce His<sub>6</sub>-tag at the C-terminus of each fragment.

**Purification of  $\alpha$ ,  $\beta$ , and  $\beta'$  Subunits, and  $\beta$  Fragments.** Subunits  $\alpha$ ,  $\beta$ , and  $\beta'$  were expressed using pGEMA185 (6), pGETB (see above), and pGETC (see above), respectively. *E. coli* BL21(DE3) was used for expression of  $\alpha$  and  $\beta$ , while *E. coli* JM109(DE3) was used for expression of  $\beta'$  because pGETC failed to transform strain BL21(DE3). Fragments of the  $\beta$  subunit were expressed in strain BL21(DE3) using the respective expression plasmids constructed as above. The intact  $\beta$  and  $\beta'$  subunits and the recombinant  $\beta$  fragments were all recovered in inclusion bodies of cell extracts. The proteins were solubilized with a dissociation buffer (50 mM Tris-HCl, pH 8.0, at 4 °C, 0.2 M KCl, 10 mM MgCl<sub>2</sub>, 1 mM EDTA, 10 mM dithiothreitol (DTT), 20%(v/v) glycerol, and 6 M urea) and centrifuged at 100000g for 2 h at 4 °C. The supernatant was subjected to DEAE-TOYOPEARL 650M (TOSOH) column chromatography, and proteins were eluted with a linear gradient of 50 mM to 0.5 M NaCl in TGED (10 mM Tris-HCl, pH 8.0, at 4 °C, 5%(v/v) glycerol, 0.1 mM EDTA, and 0.1 mM DTT) containing 6 M urea. The eluate was then fractionated by Hi-trap Heparin (Pharmacia Biotech) column chromatography. The purified subunits were dialyzed against a storage buffer (10 mM Tris-HCl, pH 7.6, at 4 °C, 10 mM MgCl<sub>2</sub>, 0.2 M KCl, 0.1 mM EDTA, 1 mM DTT, and 50%(v/v) glycerol) and stored at –30 °C until use.

**Reconstitution of the  $\alpha_2\beta$  Complex and Core Enzyme.** Reconstitution of  $\alpha_2\beta$  complex and core enzyme was carried out as described in Fujita and Ishihama (20). Isolated  $\beta$  or  $\beta'$  fragments were mixed with purified  $\alpha$  ( $\alpha$ : $\beta$  molar ratio = 2:1) or a mixture of  $\alpha$  and  $\beta'$  subunits ( $\alpha$ : $\beta$ : $\beta'$  molar ratio = 2:1:1) in the dissociation buffer. Urea was removed by dialysis against the standard reconstitution buffer (50 mM Tris-HCl, pH 8.0, at 4 °C, 0.3 M KCl, 10 mM MgCl<sub>2</sub>, 10  $\mu$ M ZnCl<sub>2</sub>, 0.1 mM EDTA, 1 mM DTT, and 20%(v/v) glycerol).

**Trypsin Cleavage.** Limited proteolysis by trypsin was performed according to Negishi et al. (11). In brief, the isolated  $\beta$  subunit (0.13 mg/mL) or the  $\alpha_2\beta$  complex (0.20 mg/mL) in a cleavage buffer (40 mM Tris-HCl, pH 7.8, 40 mM KCl, and 5% glycerol) were preincubated at 37 °C for 3 min and then subjected to trypsin cleavage at an input trypsin– $\beta$  subunit ratio of 1:3000 (w/w). After incubation for 5 min at 37 °C, the reaction was terminated by adding phenylmethylsulfonylfluoride (PMSF) at a final concentration of 5 mM.

**Determination of N-Terminal Amino Acid Sequences.** N-terminal amino acid sequences of  $\beta$  fragments were determined as described by Negishi et al. (11). In brief, proteins in gels were blotted onto PVDF (poly(vinylidene difluoride))-type supports (ProBlott, Applied Biosystems) and the membranes were stained with Coomassie brilliant blue R-250. Stained protein bands were cut from the membranes and directly subjected to Edman degradation analysis using an Applied Biosystems model 491 Protein Sequencer.

**Ni<sup>2+</sup>-NTA Agarose-Binding Assay.** Batch-mode Ni<sup>2+</sup> affinity chromatography was performed as described in Tang et al. (21). In brief, 1 nmol of  $\alpha$  and 0.5 nmol each of  $\beta$  (or  $\beta$  fragments) and  $\beta'$  subunit were mixed together in the dissociation buffer and then subjected to reconstitution as

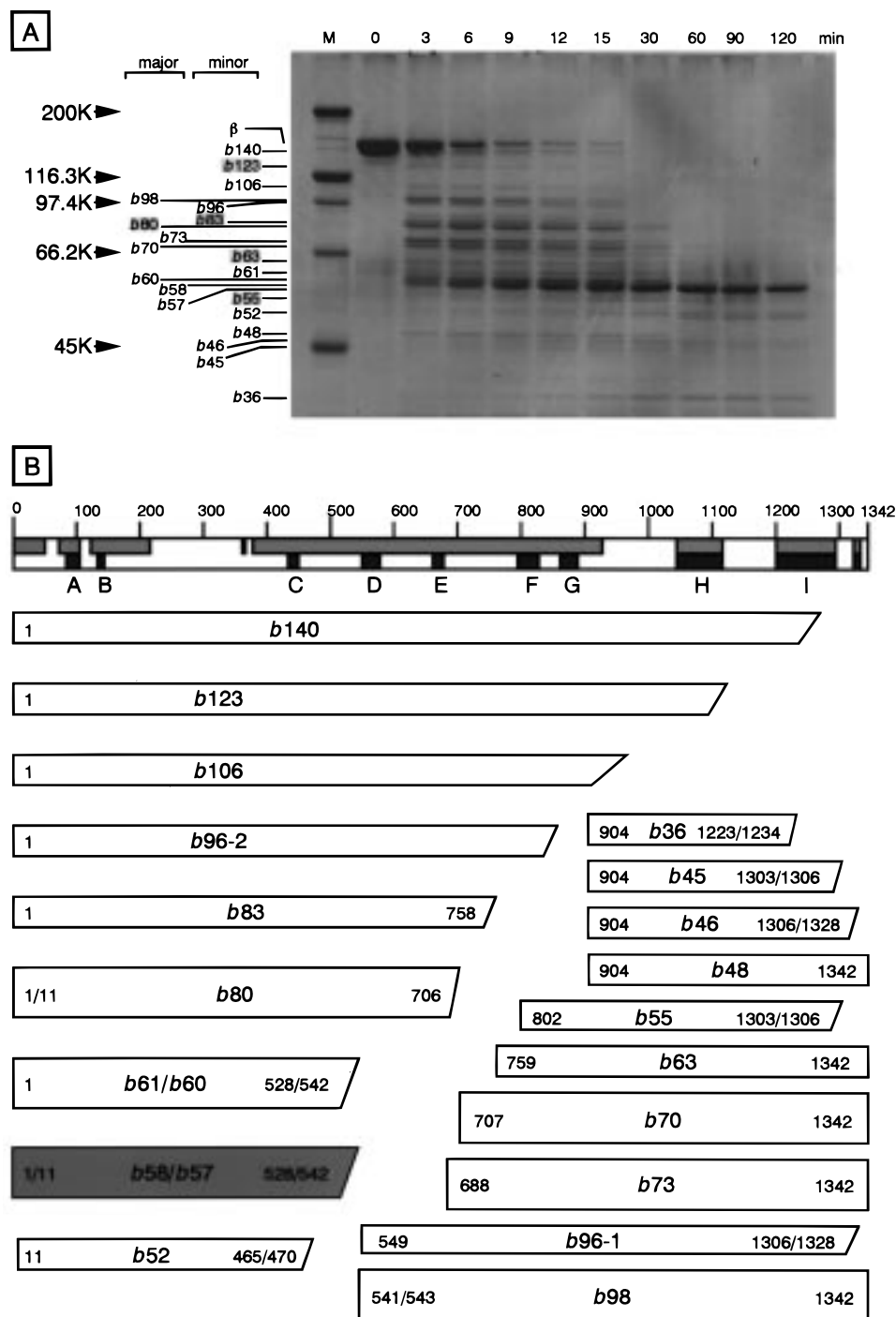


FIGURE 1: Tryptic cleavage of the  $\beta$  subunit. (A) Isolated  $\beta$  subunit (130  $\mu\text{g/mL}$ ) was treated at 37  $^{\circ}\text{C}$  with 0.043  $\mu\text{g/mL}$  of trypsin in a cleavage buffer (40 mM Tris-HCl, pH 7.8, at 37  $^{\circ}\text{C}$ , 40 mM KCl and 5% glycerol). At various times indicated, aliquots of 20  $\mu\text{L}$  were subjected to SDS-7.5% PAGE. Proteins were blotted onto PVDF membranes followed by staining with Coomassie blue R-250. The bands are designated on the basis of the molecular weight estimated from the migration distance on SDS-PAGE. The shaded components represent those identified only for the  $\beta$  subunit but not for the  $\alpha\beta$  complex (see Figure 3). (B) Stained protein bands on PVDF membranes were cut out and subjected to N-terminal amino acid sequencing according to Negishi et al. (11). From the N-terminal amino acid sequences, the tryptic fragments indicated in panel A are aligned along the sequence of the  $\beta$  subunit. The sites of C-terminal ends were estimated from the fragment sizes and the location of potential cleavage sites by trypsin. Major products are shown by wider bars. The b58/b57 fragments are the most abundant products after prolonged treatment with trypsin.

described but in the absence of DTT. To the reconstituted subunit mixture, 0.2 mL of  $\text{Ni}^{2+}$ -NTA agarose (Qiagen) previously equilibrated with buffer D (50 mM Tris-HCl, pH 7.9, at 4  $^{\circ}\text{C}$ , 0.1 mM EDTA and 5% (v/v) glycerol) plus 5 mM imidazole was added and incubated for 30 min at 4  $^{\circ}\text{C}$ . Agarose beads were washed with 0.3 mL of buffer D plus 5 and 25 mM imidazole, and then the proteins were eluted

with 0.3 mL of buffer D plus 200 mM imidazole. Each fraction was analyzed by 7.5% SDS-PAGE.

## RESULTS AND DISCUSSION

*Limited Proteolysis of the Isolated  $\beta$  Subunit.* The  $\beta$  subunit of *E. coli* RNA polymerase consists of 1342 amino acid residues and contains a total of 170 potential cleavage



sites by trypsin. Limited digestion of the isolated  $\beta$  subunit was carried out at various trypsin concentrations and for various times. Figure 1A shows a time-dependent change in the cleavage pattern. The major cleavage products are designated on the basis of apparent molecular size estimated from the mobility on SDS–PAGE (the fragments with symbols *b* and *ab* represent those derived from the free  $\beta$  subunit and the  $\alpha_2\beta$  complex, respectively, while the numbers following the symbols represent the molecular sizes estimated from the migration distance on SDS–PAGE). After analysis of the N-terminal amino acid sequences, the sites of trypsin cleavage were determined for all of these major tryptic fragments, while the C-termini of these fragments were estimated from the fragment sizes and the location of potential trypsin cleavage sites. Figure 1B shows the locations of major tryptic fragments thus estimated along the primary sequence of  $\beta$  subunit (the major fragments as identified by staining intensity are shown by wider bars).

The initial trypsin cleavage takes place at residues R540/R542, R687, and R706 in the central part of  $\beta$  subunit (Figure 1B), generating N-terminal fragments *b58/b57*, *b80*, and *b83*, and C-terminal fragments *b98*, *b73*, and *b70*. In the case of assembled core enzyme, the most sensitive sites for tryptic cleavage of the  $\beta$  subunit are located at either R905 or K909 (22), but the cleavage at these sites of isolated  $\beta$  subunit was found to take place only after the initial cleavages, indicating that the conformation of  $\beta$  subunit is different between the unassembled  $\beta$  subunit and that assembled in the RNA polymerase.

**Identification of the N-Terminal Structural Domain.** Among the N-terminal fragments generated by a single and the first cut by trypsin, the fragments *b58/b57* are relatively resistant to trypsin even after prolonged incubation and become the most abundant component at 120 min (see Figure 1A), indicating that the N-terminal segment forms a protease-insensitive structural domain. After N-terminal sequencing, the *b58/b57* was found to be the fragments from residue 1 down to about residues 528–542. The N-terminal fragments (*b140*, *b123*, *b106*, *b96–2*, *b83*, *b80*, and *b61/b62*) larger than *b58/b57* disappeared in a time-dependent manner. Besides the *b58/b57* fragment, an N-terminal fragment *b52* with the sequence of residues 11 to 465/470, lacking short segments from both N- and C-termini of *b58/b57* (see Figure 1B), increased concomitantly with the increase in time of trypsin treatment, indicating that this fragment is a secondary product generated from the larger N-terminal fragments. The level of this *b52* fragment was lower than those of the major fragments *b58/b57* (see Figure 1A).

The N-terminal *b58/b57* domains include the regions A, B, and C conserved among  $\beta$  homologues from not only prokaryotic but also eukaryotic RNA polymerases (23, 24) and the N-terminal-proximal dispensable region (the dispensable region I) between the conserved regions B and C (25). However, no specific function has yet been identified for these N-terminal-proximal regions, except that the region B is one of the four regions forming the binding site of rifampicin (26) and a short deletion in the region C leads to a decrease in the binding activity of RNA polymerase to DNA (27).

**Identification of the C-Terminal Structural Domain.** In the initial period of trypsin cleavage, we identified at least six C-terminal fragments, *b98* (cleaved at 540/542), *b96–1*

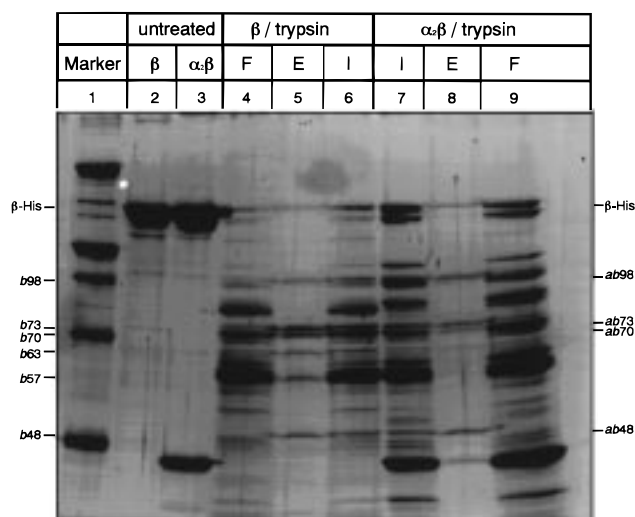


FIGURE 2: Isolation of C-terminal fragments of the  $\beta$  subunit. The  $\beta$  subunit with His<sub>6</sub>-tag at its C-terminus (lane 2) and the  $\alpha_2\beta$  complex containing the His<sub>6</sub>-tagged  $\beta$  subunit (lane 3) were prepared as described in Materials and Methods. Both the  $\beta$  subunit (lanes 4–6) and the  $\alpha_2\beta$  complex (lanes 7–9) were subjected to tryptic digestion under the same conditions as described in Figure 1, and then mixed with Ni<sup>2+</sup>-NTA agarose resin. After being washed with a buffer containing 6 M urea, the resin-bound  $\beta$  fragments were eluted with an elution buffer containing 200 mM imidazole. Fractions were analyzed by SDS–7.5% PAGE: I (lanes 6 and 7), input samples; F (lanes 4 and 9), flow-through fractions; E (lanes 5 and 8), fractions eluted with imidazole. The resin-bound fragments are shown on the right side (see Figure 3 for the identification of *ab* fragments) while the location of fragments generated from the His<sub>6</sub>-tagged  $\beta$  subunit are indicated on the left side (see Figure 1 for the identification of *b* fragments).

(cleaved at 548), *b73* (cleaved at 687), *b70* (cleaved at 706), *b63* (cleaved at 758), and *b48* (cleaved at 903) (Figure 1A). These fragments except for *b96–1* retain the  $\beta$ -subunit C-terminal sequence for 10–15 min of the incubation (see below). These C-terminal fragments except for *b48* include the conserved regions F, G, H, and I and the C-terminal-proximal dispensable region (the dispensable region II) between regions G and H (28, 29). The catalytic site for RNA polymerization is believed to include regions H and I because the initiation nucleotides and 3' ends of the nascent RNA can be cross-linked to these regions (30, 31). These C-terminal large fragments (*b98*, *b96–1*, *b73*, *b70*, and *b63*) are, however, unstable and rapidly degraded until 15 min (Figure 1A). Concomitantly with the decrease of these large C-terminal fragments, fragment *b55* (cleaved at 801) and at least three smaller fragments, *b46*, *b45*, and *b36*, all carrying the same N-terminal sequence (after residue 904), increased in a time-dependent manner, suggesting that these smaller fragments are generated by the secondary cleavage within the C-terminal-proximal region. Within the range of analysis, the smallest C-terminal fragment *b36* (residues 904–1223/1234) appeared at 30 min of the trypsin digestion and stayed at least until 120 min (see Figure 1A).

The protease-sensitive central part of the  $\beta$  subunit between residues R540/R542 and R801 includes the conserved regions D and E. It should be worthwhile to note that the binding sites for rifampicin (32, 33), streptolydigin (34), priming substrates (30, 35), and the stringent factor ppGpp (36, 37) are all clustered in this protease-sensitive and supposedly surface-exposed region. Furthermore, one of the two contact

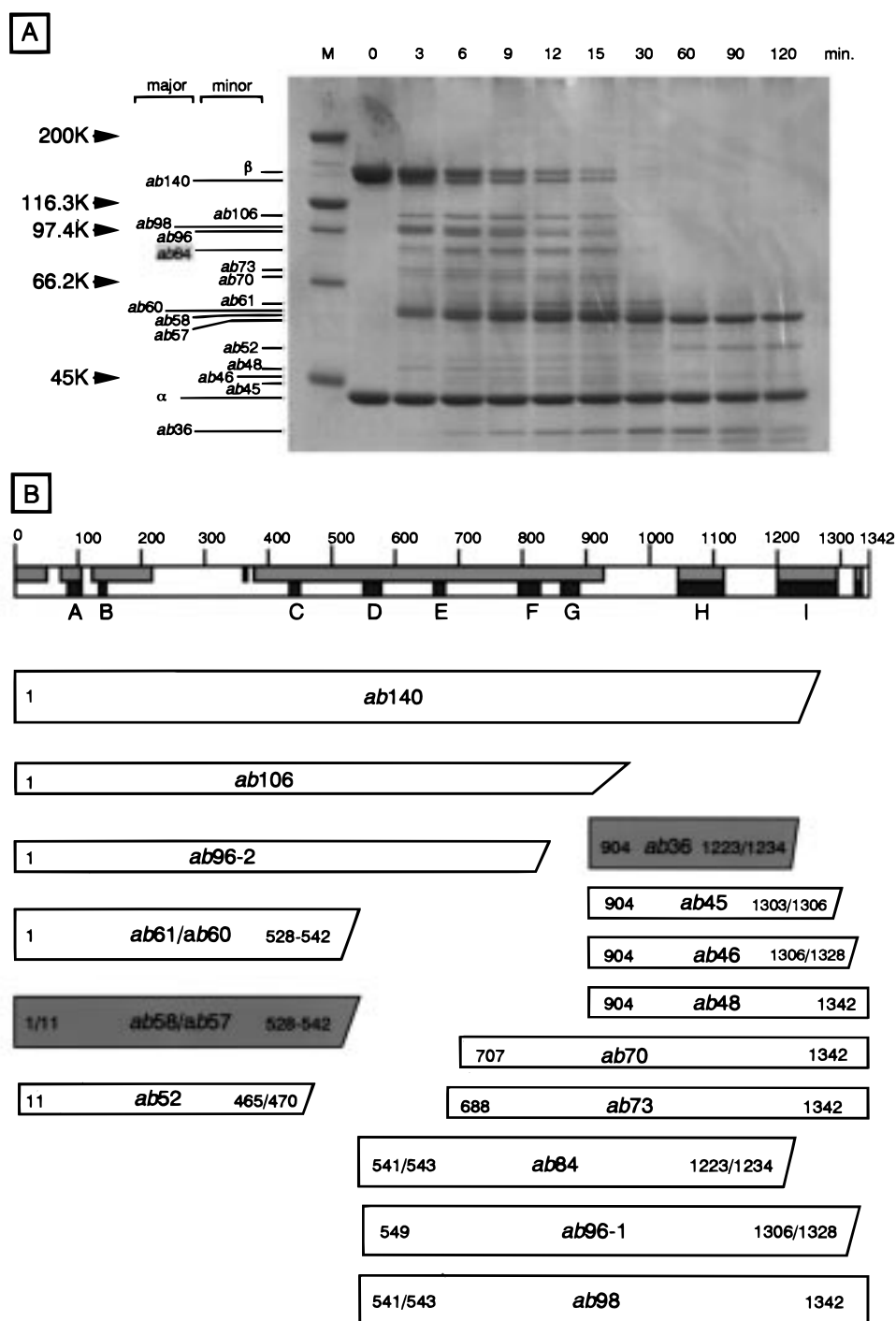


FIGURE 3: Trypsin cleavage of the  $\alpha_2\beta$  complex. (A) Reconstituted and purified  $\alpha_2\beta$  complex (200  $\mu\text{g}/\text{mL}$ ) was treated at 37 °C with 0.043  $\mu\text{g}/\text{mL}$  trypsin in a cleavage buffer (40 mM Tris-HCl, pH 7.8, at 37 °C, 40 mM KCl and 5% glycerol). At various times indicated, aliquots of 20  $\mu\text{L}$  were subjected to SDS-7.5% PAGE. Proteins were blotted onto PVDF membranes followed by staining with Coomassie blue R-250. The bands are designated on the basis of the molecular weight estimated from the migration distance on SDS-PAGE. The shadowed components represent those identified only for the  $\alpha_2\beta$  complex but not for the  $\beta$  subunit (see Figure 1). (B) N-terminal amino acid sequences were determined for the major tryptic products according to Negishi et al. (11). From the N-terminal amino acid sequences, the tryptic fragments are aligned along the sequence of the  $\beta$  subunit. The sites of C-terminal ends were estimated from the fragment sizes and the location of potential cleavage sites by trypsin. Major products are shown by wider bars.

sites of the  $\sigma^{70}$  subunit on  $\beta$  is also located in this region (38). Accordingly a number of mutations affecting transcription pausing and termination have been mapped in this region, mostly overlapping with the rifampicin-binding site (39, 40), and some RNA polymerase mutants which are unable to support bacterial growth carry mutations in these regions (41).

*Limited Proteolysis of the His<sub>6</sub>-Tagged  $\beta$  Subunit.* To identify the fragments carrying the C-terminal sequence of  $\beta$  subunit down to the terminal amino acid residue, we prepared the  $\beta$  subunit fused to the His<sub>6</sub> tag at the C-terminus and carried out limited trypsin digestion experiments for the purified His<sub>6</sub>-tagged  $\beta$  subunit under the same conditions as above. After trypsin treatment, C-terminal fragments with

the His<sub>6</sub> tag were bound to Ni<sup>2+</sup>-NTA agarose resin and the resin-bound proteins were washed with a buffer containing 6 M urea to remove associated fragments of the  $\beta$  subunit, and then eluted with imidazole. At least six fragments were isolated (Figure 2, lane 5). From the N-terminal sequences, five were found to correspond to *b*98, *b*73, *b*70, *b*63, and *b*48 (see Figure 1B), confirming that all these five fragments represent the products generated by the initial cleavage of  $\beta$  subunit with trypsin.

By using the His<sub>6</sub>-tagged  $\beta$  subunit, we identified one more C-terminal fragment, which migrated between His-tagged *b*63 and *b*48 (Figure 2, lane 5). The corresponding C-terminal fragment without His<sub>6</sub>-tag might overlap with the major N-terminal fragment *b*58/*b*57 on SDS–PAGE (see Figure 1A). Otherwise the C-terminal *b*57 fragment might be rapidly converted into *b*55 after the secondary cleavage within the C-terminal-proximal region (see Figure 1B).

**Limited Proteolysis of the  $\alpha_2\beta$  Complex.** The  $\alpha_2\beta$  complex is the stable intermediate in both in vitro and in vivo assembly of the RNA polymerase (1). As an attempt for determination of the contact site(s) of  $\alpha$  subunit on the  $\beta$  subunit, we reconstituted the  $\alpha_2\beta$  complex from isolated individual subunits. The reconstituted  $\alpha_2\beta$  complex is fully active in forming the  $\alpha_2\beta\beta'$  core enzyme with the catalytic activity of RNA polymerization (1, 20). We carried out limited trypsin digestion of the isolated  $\alpha_2\beta$  complex, and the time-dependent change of SDS–PAGE patterns is shown in Figure 3A (the fragments derived from the  $\alpha_2\beta$  complex are all indicated by the symbol *ab* followed by the apparent molecular weights). The origins of tryptic fragments were identified by the N-terminal sequencing. The  $\alpha$  subunit is less sensitive to trypsin than  $\beta\beta'$  subunits in the assembled core enzyme (42) and under isolated states (11). Although all fragments migrating slower than the  $\alpha$  subunit on SDS–PAGE should therefore be derived from the  $\beta$  subunit, we confirmed the origin of each fragment by N-terminal sequencing.

Figure 3B shows the location of the major fragments of  $\beta$  subunit derived from the  $\alpha_2\beta$  complex along the map of  $\beta$  subunit. A significant difference was observed in the cleavage pattern between the isolated free  $\beta$  subunit and the  $\beta$  subunit within the  $\alpha_2\beta$  complex (compare Figure 1 and Figure 3), in particular in the central part. The initial tryptic cleavage sites R758 and R801 for the unassembled free  $\beta$  subunit became resistant in the  $\alpha_2\beta$  complex, implying that these sites are protected from trypsin digestion by binding of the  $\alpha$  subunit. The levels of *ab*73 (residues 688–1342) and *ab*70 (residues 707–1342) are also lower than those of *b*73 and *b*70, suggesting that the sites 687 and 707 of the  $\beta$  subunit in the  $\alpha_2\beta$  complex also became less sensitive to trypsin than in the unassembled free  $\beta$  subunit. Instead the cleavage at residues R1223/K1234 was enhanced in the  $\alpha_2\beta$  complex, suggesting that the extreme C-terminal part became sensitive to trypsin. As in the case of *b*58/*b*57 (residues 1/11–503/529) derived from the free  $\beta$  subunit, the N-terminal fragments *ab*58/*ab*57 (residues 1/11–503/529) were resistant to trypsin digestion.

For identification of the C-terminal fragments generated by the initial trypsin cleavage, we also carried out limited digestion of the  $\alpha_2\beta$  complex consisting of His<sub>6</sub>-tagged  $\beta$ . After affinity absorption of the trypsin-treated  $\alpha_2\beta$  complex to Ni<sup>2+</sup>-NTA resin under the denatured conditions, we

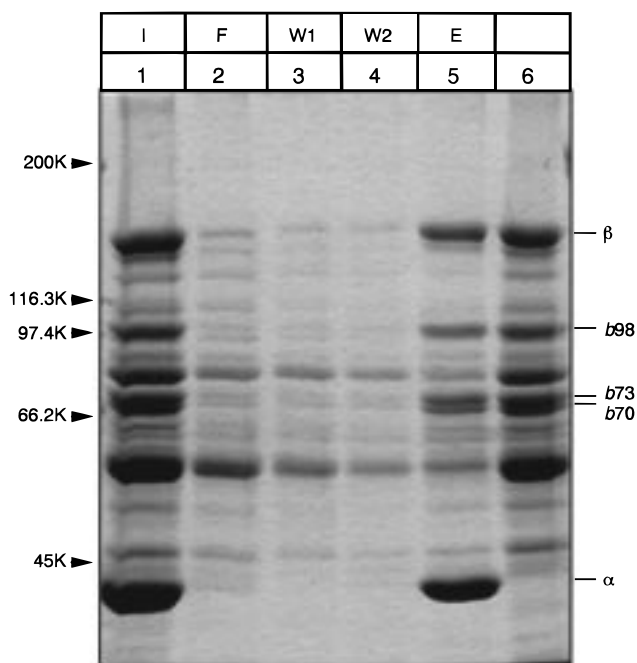


FIGURE 4: Complex formation between the His<sub>6</sub>-tagged intact  $\alpha$  subunit and various  $\beta$  fragments. Trypsin-treated  $\beta$  subunit (80  $\mu$ g) was mixed with the purified His<sub>6</sub>-tagged  $\alpha$  (60  $\mu$ g) in the dissociation buffer. After removal of urea by dialysis against the standard reconstitution buffer, the mixture was mixed with Ni<sup>2+</sup>-NTA affinity resin. The resin-bound proteins were eluted with increasing concentrations of imidazole: lane 1, the applied sample (trypsin-treated  $\beta$  subunit plus His-tagged  $\alpha$ ); lane 2, unbound fraction; lane 3, 5 mM imidazole eluate; lane 4, 25 mM imidazole eluate; lane 5, 200 mM imidazole eluate; lane 6, trypsin-treated  $\beta$  subunit. The locations of major tryptic fragments of the  $\beta$  subunit are shown on right, while those of marker proteins are shown on left.

identified three fragments (*ab*98, *ab*73, and *ab*70) which correspond to *b*98, *b*73, and *b*70, but failed to detect other two fragments corresponding to *b*63 and *b*57 (see Figure 2, lane 8). This observation confirms our prediction that the two sites, residues R758 and R801, become resistant to trypsin digestion after the  $\alpha_2\beta$  complex formation.

The results altogether suggest that (i) the  $\alpha$  subunit associates at the central part of  $\beta$  subunit (including R758 and R801) and thereby this region is protected from tryptic digestion; and (ii) the association of  $\alpha$  at the central portion alters the extreme C-terminal portion sensitive to trypsin. The putative  $\alpha$  subunit contact site includes the conserved region F and its upstream sequence. However, it is not excluded yet that the  $\alpha$  binding at a site other than the central part induces the conformational change in  $\beta$  so as to make the central part resistant to trypsin digestion.

**Formation of Binary Complexes between the His<sub>6</sub>-Tagged  $\alpha$  Subunit and Various  $\beta$  Fragments.** To confirm the above interpretation, we examined the formation of binary complexes between the intact  $\alpha$  subunit and various  $\beta$  fragments. For this purpose, we isolated the  $\alpha$  subunit with His<sub>6</sub>-tag at its C-terminus as described previously (17) and combined it with a mixture of trypsin-treated  $\beta$  subunit fragments under the denatured condition. The addition of His<sub>6</sub>-tag at C-terminus does not interfere with the assembly activity of wild-type  $\alpha$  subunit [however, some  $\alpha$  mutants become inactive in the assembly by the addition of His-tag (17)] and with the enzymatic activity of assembled core enzyme.

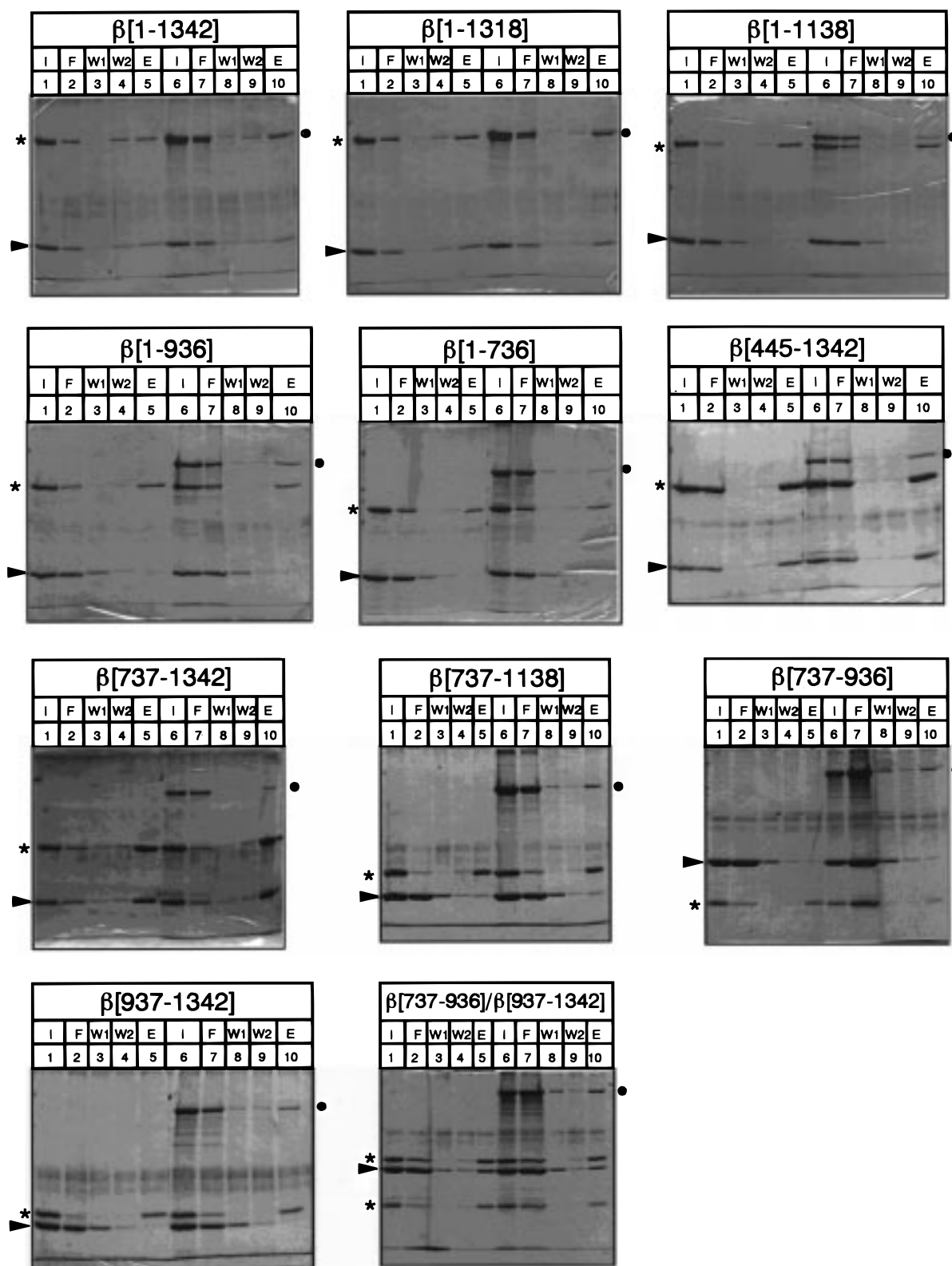


FIGURE 5: Formation of the  $\alpha_2\beta$  and  $\alpha_2\beta\beta'$  complexes using the His<sub>6</sub>-tagged  $\beta$  fragments. Each of the purified His<sub>6</sub>-tagged  $\beta$  fragments (0.5 nmol each) was mixed with either the  $\alpha$  subunit (1 nmol) [lanes 1–4] or a mixture of the  $\alpha$  (1 nmol) and  $\beta'$  (0.5 nmol) subunits [lanes 5–8] in the dissociation buffer. After removal of urea by dialysis against the standard reconstitution buffer, the subunit mixtures were mixed with Ni<sup>2+</sup>-NTA affinity resin. Proteins were eluted with increasing concentrations of imidazole: lanes 1 and 5, the applied samples; lanes 2 and 6, unbound fractions; lanes 3 and 7, 5 mM imidazole eluate; lanes 4 and 8, 200 mM imidazole eluate. Arrowheads on the left indicate the  $\alpha$  subunit, while stars on left indicate the position of His<sub>6</sub>-tagged  $\beta$  subunit fragments. Dots on right indicate the migration position of the  $\beta'$  subunit.

Mixtures of the His<sub>6</sub>-tagged  $\alpha$  and various  $\beta$  fragments in the denaturation buffer containing 6 M urea were dialyzed under the same condition as that employed for the  $\alpha_2\beta$

complex formation in vitro (20);  $\alpha$ - $\beta$  fragment complexes thus formed were isolated by Ni<sup>2+</sup>-NTA affinity chromatography.



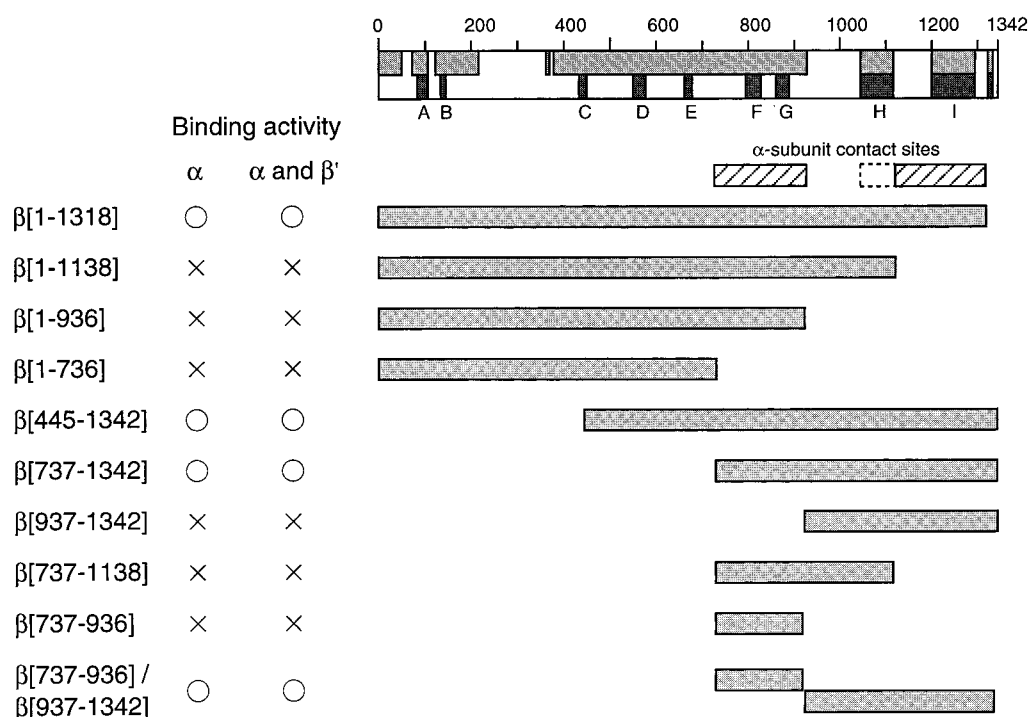


FIGURE 6: The subunit–subunit contact sites on the  $\beta$  subunit. Fragments of the  $\beta$  subunit examined for the binding assays with  $\alpha$  and  $\beta'$  subunits are shown along the map of intact  $\beta$  subunit. The activities of the complex formation with either  $\alpha$  subunit ( $\alpha$ – $\beta$  fragment complexes) or both  $\alpha$  and  $\beta'$  subunits ( $\alpha$ – $\beta$  fragment– $\beta'$  complexes or pseudo-core complexes) are indicated for each of the indicated  $\beta$  fragments (O, active; X, inactive). We propose two contact regions on the  $\beta$  subunit with the  $\alpha$  subunit. Reservation is made for the possible involvement of the conserved region H (see text).

All of the N-terminal fragments of  $\beta$  upstream from the initial cleavage sites failed to form binary complexes with the  $\alpha$  subunit and were recovered in the unbound flow-through fractions (Figure 4). On the other hand, the C-terminal large fragments, *b*98 (residues 541/543–1342), *b*96–1 (549–1306/1328), *b*73 (688–1342), and *b*70 (707–1342) (see Figure 1B), all including the putative  $\alpha$ -contact site in the central part of  $\beta$  predicted from the tryptic cleavage experiments (see above), were recovered in the complex fractions, which were eluted only in the presence of high concentrations of imidazole (Figure 4, lane 5). None of these  $\beta$  subunit fragments were found to bind to the  $\text{Ni}^{2+}$ -NTA resin in the absence of  $\alpha$  subunit. These results indicate that the primary contact site(s) on the  $\beta$  subunit with the  $\alpha$  subunit is(are) located in the C-terminal half at a site(s) downstream from residue A707.

**Formation of Binary Complexes between the  $\alpha$  Subunit and His<sub>6</sub>-Tagged  $\beta$  Fragments.** To confirm this result and to narrow down the  $\alpha$  contact site on  $\beta$ , we also carried out the same type of binary complex formation experiment, but using the intact  $\alpha$  subunit and His<sub>6</sub>-tagged  $\beta$  fragments. For this purpose, a set of expression plasmids was constructed, which overexpressed a total of 15 recombinant  $\beta$  subunit fragments, that is, six C-terminal truncated fragments, five N-terminal truncated fragments, and four internal fragments, each containing a C-terminal His<sub>6</sub>-tag (see Figure 6 for the map of fragments). All of these His<sub>6</sub>-tagged  $\beta$  subunit fragments were purified from inclusion bodies of the expressed cell extracts in the presence of urea and mixed with the purified  $\alpha$  subunit under the denatured condition. Binary complexes formed after renaturation were isolated by  $\text{Ni}^{2+}$ -NTA affinity chromatography and analyzed by

SDS–PAGE. The elution patterns from  $\text{Ni}^{2+}$ -NTA affinity columns are shown in Figure 5.

One large N-terminal fragment  $\beta(1-1318)$  and two C-terminal fragments,  $\beta(445-1342)$  and  $\beta(737-1342)$ , formed the binary complexes with the  $\alpha$  subunit. The efficiency of binary complex formation of these  $\beta$  fragments was as high as that of the intact  $\beta$  subunit, indicating that the primary contact site for  $\alpha$  is located downstream between residues 737 and 1342. On the basis of the tryptic cleavage maps, we predicted the  $\alpha$  contact site on the  $\beta$  subunit is located in the central part including residues R687, R758, and R801 (see above), but the fragment  $\beta(737-936)$  alone was apparently inactive in the formation of a stable complex with the  $\alpha$  subunit. Likewise, the fragment  $\beta(937-1342)$  alone was inactive in the binding of  $\alpha$  subunit. Thus, a sequence(s) of  $\beta$  downstream from R937 was considered to be required for the tight binding of the primary contact site of  $\beta$  with  $\alpha$ . We then tested the possible influence of the  $\beta$  sequence downstream from the residue R937 on the binding of  $\alpha$  subunit.

A low level of the  $\alpha$ -binding activity was detected for the fragment  $\beta(737-1138)$ , but its activity was less than one-tenth of the level of  $\beta(737-1342)$  (see Figure 5), indicating that the sequence downstream 1139 including the region I influences the  $\alpha$ -binding affinity of  $\beta$ . Since the  $\beta(1-1318)$  is fully active in  $\alpha$  binding, this secondary site for  $\alpha$  binding should be located downstream from residue A1139 but upstream from G1318. The involvement of two separate regions in the stable binding of  $\alpha$  subunit to  $\beta$  is supported by the finding that, by mixing  $\beta(737-935)$  and  $\beta(937-1342)$ , the full activity of  $\alpha$  binding was regained (see Figure 5). Since only the central part of  $\beta$  is protected from the



proteolytic cleavage after  $\alpha$  binding, we propose that the  $\beta$  region between residues A1139 and G1318 plays a regulatory role in  $\alpha$  binding, for instance, by making a transient contact with  $\alpha$  at an intermediate step during the  $\alpha_2\beta$  complex formation or by promoting proper folding of the central part of  $\beta$  as to expose the primary  $\alpha$  contact site. The involvement of the extreme C-terminal region downstream from residue A1139 may be related to the increase in protease sensitivity at residue K1234 after association with  $\alpha$  (compare Figures 1 and 3).

**Location of  $\alpha$  Subunit Contact Site(s) on the  $\beta$  Subunit.** Taken all of our observations together and as shown in Figure 6, we propose that (i) the primary contact site of  $\alpha$  subunit on the  $\beta$  subunit is located at the central portion between residues N737 and R936 including the conserved regions F and G; and (ii) the extreme C-terminal region between residues A1139 and G1318, including the conserved region I and the putative catalytic center for RNA polymerization (30, 31), plays a regulatory role in the binary complex formation. The intermediate region between these two domains for  $\alpha$  assembly may not be involved in this process because at least parts of this region (the dispensable region II) can be deleted without affecting the assembly and function of RNA polymerase (29). At present, however, we cannot exclude possible involvement of the conserved region H in a step of  $\alpha$  subunit assembly.

After analysis of  $\beta$  fragments with the binding activity to the His<sub>6</sub>-tagged  $\alpha$ , Wang et al. (19) reported that a C-terminal fragment of the  $\beta$  subunit downstream from residue 643 is able to bind the N-terminal assembly domain fragment of  $\alpha$  subunit ( $\alpha$ NTD). The two sites, one between residues N737 and R936 and the other between residues A1139 and G1318, determined in this study for the stable binding of full-sized  $\alpha$  subunit are both included in this C-terminal half of the  $\beta$  subunit. However, they also propose that the primary contact site is located in a C-terminal-proximal part between residues G907 and A1245. The discrepancy might be due to the difference in the assay of binary complex formation between  $\alpha$  and  $\beta$  fragments. For instance, Wang et al. (19) used excess amounts of the  $\beta$  fragments while we used a stoichiometric molar ratio of 2:1 for  $\alpha$ - $\beta$ . For the complex isolation from Ni<sup>2+</sup>-NTA resin, they used an elution buffer containing 0.5 M NaCl, while we used the imidazole buffer without NaCl. The addition of high concentrations of salt in the elution buffer may strengthen the association of  $\alpha$  subunit- $\beta$  fragment complexes.

Here we demonstrated that two separate regions of the  $\beta$  subunit are required for the full activity of  $\alpha$  binding. Functional sites within the RNA polymerase  $\beta$  subunit including both the active sites for RNA polymerization and the contact sites for subunit-subunit assembly are all comprised of two segments that are not contiguous in the primary sequence. One possibility is that the binding of  $\alpha$  subunit induces the gathering of these two separated regions into a single functional site. For instance, the region D-E located upstream of this primary  $\alpha$  subunit contact site with the binding activity of substrates could be assembled into a single functional site as to be closely located with the H-I regions with the putative catalytic site for RNA polymerization (34). Likewise, the close contact of two separate sequences located upstream and downstream of the primary

$\alpha$  contact site may form a single contact site with the  $\sigma^{70}$  subunit (38).

**Location of  $\beta'$  Subunit Contact Site(s) on the  $\beta$  Subunit.** As an attempt to identify the  $\beta'$  subunit contact site(s) on  $\beta$ , the assembly activity of the core enzyme was examined for various  $\beta$  fragments in the presence of both  $\alpha$  and  $\beta'$  subunits. Pseudo-core complexes consisting of  $\alpha$ ,  $\beta$  fragment, and  $\beta'$  were formed for  $\beta(1-1318)$ ,  $\beta(445-1342)$ , and  $\beta(737-1342)$ , which all retain nearly the full activity of  $\alpha$  binding (data not shown). The level of pseudo-core complex formation is much lower for  $\beta(737-1138)$  in agreement with its low level activity of  $\alpha$  binding. Thus, we conclude that the primary contact site of  $\beta'$  subunit on  $\beta$  is located close to the  $\alpha$ -subunit contact site, indicating that the binding sites for  $\alpha$  and  $\beta'$  subunits form a single and the same structural domain. After binding of the  $\beta'$  subunit, the conformation of  $\beta$  subunit is further modulated as to render the central part around R540/R542 resistant to trypsin, and concomitantly, the most sensitive sites for tryptic cleavage of the  $\beta$  subunit in the assembled RNA polymerase are shifted to R905/K909 (22).

The intrinsic functions of RNA polymerase subunits are exposed in a stepwise manner along the assembly of subunits (1). A systematic search for the activities of the pseudo-core complexes containing various  $\beta$  fragments, such as the activity of RNA polymerization and the binding activities of  $\sigma$  subunits, promoter DNA, priming nucleotides, rifampicin, and streptolydigin, might be worthwhile to get further insight into the functional map of  $\beta$  subunit.

## ACKNOWLEDGMENTS

We thank Akira Iwata and Susumu Ueda for the preparation of antibodies against each subunit of RNA polymerase.

## REFERENCES

1. Ishihama, A. (1981) *Adv. Biophys.* 14, 1-35.
2. Fukuda, R., and Ishihama, A. (1974) *J. Mol. Biol.* 87, 523-540.
3. Ishihama, A. (1972) *Biochemistry* 11, 1250-1258.
4. Hayward, R., Igarashi, K., and Ishihama, A. (1991) *J. Mol. Biol.* 221, 23-29.
5. Igarashi, K., Fujita, N., and Ishihama, A. (1991) *J. Mol. Biol.* 218, 1-6.
6. Igarashi, K., and Ishihama, A. (1991) *Cell* 65, 1015-1022.
7. Ishihama, A. (1993) *J. Bacteriol.* 175, 2483-2489.
8. Ebright, R. H., and Busby, S. (1995) *Curr. Opin. Genet. Dev.* 5, 197-203.
9. Ishihama, A. (1997) in *Nucleic Acids & Molecular Biology, Mechanism of Transcription* (Eckstein, F., Lilley, D., Eds.) Vol. 11, pp 53-70, Springer-Verlag, Heidelberg, Germany.
10. Blatter, E. E., Ross, W., Tang, H., Gourse, R. L., and Ebright, R. H. (1994) *Cell* 78, 889-896.
11. Negishi, T., Fujita, N., and Ishihama, A. (1995) *J. Mol. Biol.* 248, 723-728.
12. Jeon, Y. H., Negishi, T., Shirakawa, M., Yamazaki, M., Fujita, N., Ishihama, A., and Kyogoku, Y. (1995) *Science* 270, 1495-1497.
13. Gaal, T., Ross, W., Blatter, E. E., Tang, H., Jia, X., Krishnan, V. V., Assa-Munt, N., Ebright, R. H., and Gourse, R. L. (1996) *Genes Dev.* 10, 16-26.
14. Jeon, Y. H., Yamazaki, T., Otomo, T., Ishihama, A., and Kyogoku, Y. (1997) *J. Mol. Biol.* 267, 953-962.
15. Kimura, M., Fujita, N., and Ishihama, A. (1994) *J. Mol. Biol.* 242, 107-115.
16. Kimura, M., and Ishihama, A. (1995) *J. Mol. Biol.* 248, 756-767.

17. Kimura, M., and Ishihama, A. (1995) *J. Mol. Biol.* 254, 342–349.
18. Miyake, R., Murakami, K., Owens, J. T., Greiner, D. P., Ozoline, O. N., Ishihama, A., and Meares, C. F. (1998) *Biochemistry* 37, 1344–1349.
19. Wang, Y., Severinov, K., Loizos, N., Fenyo, D., Heyduk, E., Heyduck, T., Chait, B. T., and Darst, S. A. (1997) *J. Mol. Biol.* 270, 648–662.
20. Fujita, N., and Ishihama, A. (1996) in *Methods in Enzymology, RNA Polymerase and Associated Factors, Part A* (Adhya, S., Ed.) pp 121–130, Vol. 273, Academic Press, San Diego, CA.
21. Tang, H., Severinov, K., Goldfarb, A., and Ebright, R. H. (1995) *Proc. Natl. Acad. Sci. U.S.A.* 92, 4902–4906.
22. Severinov, K., Mustaev, A., Kashlev, M., Borukhov, S., Nikiforov, V., and Goldfarb, A. (1992) *J. Biol. Chem.* 267, 12813–12819.
23. Sweetser, D., Nonet, M., and Young, R. A. (1987) *Proc. Natl. Acad. Sci. U.S.A.* 84, 1192–1196.
24. Coggins, J. R., Lumsden, J., and Malcolm, A. D. B. (1977) *Biochemistry* 16, 1111–1116.
25. Severinov, K., Kashlev, M., Severinova, E., Bass, I., McWilliams, K., Kutter, E., Nikiforov, V., Snyder, L., and Goldfarb, A. (1994) *J. Biol. Chem.* 269, 14254–14259.
26. Severinov, K., Soushko, M., Goldfarb, A., and Nikiforov, V. (1994) *Mol. Gen. Genet.* 244, 120–126.
27. Martin, E., Sagitov, V., Burova, E., Nikiforov, V., and Goldfarb, A. (1992) *J. Biol. Chem.* 267, 20175–20180.
28. Nene, V., and Glass, R. E. (1984) *Mol. Gen. Genet.* 196, 64–67.
29. Borukhov, S., Severinov, K., Kashlev, M., Lebedev, A., Bass, I., Rowland, G. C., Lim, P. P., Glass, R. E., Nikiforov, V., and Goldfarb, A. (1991) *J. Biol. Chem.* 266, 23921–23926.
30. Mustaev, A., Kashlev, M., Lee, J. Y., Polyakov, A., Lebedev, A., Zalenskaya, K., Grachev, M., Goldfarb, A., and Nikiforov, V. (1991) *J. Biol. Chem.* 266, 23927–23931.
31. Grachev, M. A., Lukhtanov, E. A., Mustaev, A. A., Zaychikov, E. F., Abdukayumov, M. N., Rabinov, I. V., Richter, V. I., Skloblov, Y. S., and Chisyakov, P. G. (1989) *Eur. J. Biochem.* 180, 577–585.
32. Jin, D. J., and Gross, C. A. (1988) *J. Mol. Biol.* 202, 45–58.
33. Severinov, K., Mustaev, A., Severinova, E., Kozlov, M., Darst, S. A., and Goldfarb, A. (1995) *J. Biol. Chem.* 270, 29428–29432.
34. Heisler, L. M., Suzuki, H., Landick, R., and Gross, C. A. (1993) *J. Biol. Chem.* 268, 25369–25375.
35. Mustaev, A., Zaychikov, E., Severinov, K., Kashlev, M., Polyakov, A., Nikiforov, V., and Goldfarb, A. (1994) *Proc. Natl. Acad. Sci. U.S.A.* 91, 12036–12040.
36. Glass, R. E., Jones, S. T., and Ishihama, A. (1986) *Mol. Gen. Genet.* 203, 265–268.
37. Chatterji, D., Fujita, N., and Ishihama, A. (1998) *Genes Cells* 3, 279–287.
38. Owens, J. T., Miyake, R., Murakami, K., Fujita, N., Chmura, A. J., Ishihama, A., and Meares, C. F. (1998) *Proc. Natl. Acad. Sci. U.S.A.* 95, 6021–6026.
39. Jin, D. J., Walter, W. A., and Gross, C. A. (1988) *J. Mol. Biol.* 202, 245–253.
40. Landick, R., Stewart, J., and Lee, D. N. (1990) *Genes Dev.* 4, 1623–1636.
41. Tavormina, P. L., Landick, R., and Gross, C. A. (1996) *J. Bacteriol.* 178, 5263–5271.
42. Ishihama, A., Fujita, N., and Glass, R. E. (1987) *Proteins: Struct., Funct., Genet.* 2, 42–53.

BI982381N